International Journal of Environmental Science and Technology (2026) 23:2
https://doi.org/10.1007/s13762-025-06779-6

ORIGINAL PAPER

From past to future: simulating land use and land cover changes using CA-Markov and multi-temporal satellite data

S. Keleş[1] · F. Sivrikaya[2] · A. Günlü[1]

Received: 12 August 2025 / Revised: 16 October 2025 / Accepted: 11 November 2025 / Published online: 22 November 2025

Abstract

Understanding land use and land cover (LULC) dynamics is essential for sustainable environmental management and spatial planning. This study applied the Cellular Automata–Markov (CA–Markov) model integrated with multi-temporal Landsat imagery (TM, ETM+, and OLI) to analyze past changes and project future LULC transitions in the Çankırı Forest Enterprise region of Türkiye. The classified maps for 2000, 2010, and 2020 achieved high accuracy (overall accuracy up to 95.3%, Kappa = 0.92). The CA–Markov model, validated with a 91.5% similarity rate, effectively simulated spatial–temporal dynamics of agricultural expansion, urban growth, and forest alteration. Results reveal that agricultural land increased by 73.4% over two decades, mainly driven by demographic growth and economic incentives, while forest and water resources declined. Future projections for 2030 and 2040 indicate continued urban expansion and agricultural dominance, accompanied by shrinking water bodies and shifting forest distribution. These trends suggest potential challenges for agricultural sustainability and forest conservation under increasing resource pressures. By linking model-based predictions with national forest and land-use policies, this study underscores the importance of integrating spatial forecasting tools into adaptive planning strategies. The CA–Markov framework provides a reliable, interpretable, and transferable approach for regional-scale scenario generation and evidence-based environmental policy development.

Keywords Agricultural expansion · CA–Markov model · GIS · Kappa coefficient · Land use · Remote sensing

Introduction

Understanding land use and land cover (LULC) changes is critical for assessing the environmental and socio-economic impacts of human activities on the Earth's surface. These changes directly influence ecosystem services, biodiversity, climate regulation, and hydrological cycles (Foley et al. 2005). Rapid urbanization, agricultural expansion, deforestation, and infrastructure development have significantly altered natural landscapes, often leading to land degradation, habitat fragmentation, and increased greenhouse gas emissions (Lambin et al. 2001; Belay et al. 2024; Behera et al. 2025). Recent studies highlight that accelerated human-induced land transformations have intensified pressures on ecological systems, particularly in developing regions (Kavathekar et al. 2025; Tahir et al. 2025). Monitoring and analyzing LULC dynamics through advanced geospatial technologies enables policymakers, planners, and researchers to develop sustainable land management strategies, mitigate environmental risks, and ensure the resilience of ecosystems in the face of global environmental change (Turner et al. 2007; Beroho et al. 2023; Alsharif et al. 2022).

LULC change is a fundamental component of environmental transformation, directly influencing ecosystem dynamics, natural resource management, and sustainable development strategies. As global urbanization and anthropogenic pressures intensify, understanding the spatiotemporal patterns of LULC becomes crucial for informed policy-making and land use planning (Karimi et al. 2018;

Editorial responsibility: Samareh Mirkia.

✉ F. Sivrikaya
fsivrikaya@kastamonu.edu.tr

S. Keleş
sedatkeles@karatekin.edu.tr

A. Günlü
alkangunlu@karatekin.edu.tr

1 Faculty of Forestry, Department of Forestry Engineering, Çankırı Karatekin University, 18100 Kastamonu, Turkey

2 Faculty of Forestry, Department of Forestry Engineering, Kastamonu University, 37150 Kastamonu, Turkey

Moradi et al. 2020; Masalvad et al. 2024; Weslati et al. 2023; Mathewos et al. 2022). Remote sensing technologies and Geographic Information Systems (GIS) have revolutionized LULC monitoring, enabling researchers to track past changes and forecast future land transitions with high accuracy (Kumar et al. 2014; Tadese et al. 2021; Hind et al. 2022; Tariq et al. 2022; Nagasa and Edosa 2024). These technologies, particularly cloud-based systems such as Google Earth Engine, facilitate rapid processing of multi-temporal datasets for more reliable LULC classification and prediction (Belay et al. 2024; Ghalehteimouri et al. 2022).

Among predictive modeling approaches, the Cellular Automata-Markov (CA-Markov) model has gained widespread application due to its ability to simulate complex land transformation processes over time. By integrating Markov chain probability transitions with spatially explicit cellular automata rules, this model provides a dynamic framework for forecasting future LULC scenarios (Nouri et al. 2014; Aliani et al. 2019; Nasehi et al. 2019; Hind et al. 2022; Aniah et al. 2023; Asif et al. 2023; Weslati et al. 2023; Belay et al. 2024; Aksoy 2024). Several studies have demonstrated the robustness of CA-Markov in analyzing urban expansion, deforestation, agricultural intensification, and wetland degradation, offering valuable insights into land management strategies (Halmy et al. 2015; Aliani et al. 2019; Yulianto et al. 2019; Ruben et al. 2020; Huang et al. 2020; Mansour et al. 2020; Aksoy and Kaptan 2020; Bagaria et al. 2021; Khwarahm et al. 2021; Tadese et al. 2021; Rahnama 2021; Wang et al. 2021; Jana et al. 2022; Fu et al. 2022; Tariq et al. 2022; Aksoy et al. 2022; Aksoy 2024). Recent applications in Ethiopia, India, Saudi Arabia, and Iraq have shown that the CA–Markov model can effectively predict both short- and long-term landscape transformations under varying socio-economic scenarios (Alsharif et al. 2022; Khwarahm et al. 2021; Behera et al. 2025; Tahir et al. 2025). In particular, scenario-based modeling—such as “business-as-usual” versus “governance” projections—has emerged as a critical tool for assessing the impact of policy decisions on land use trends (Belay et al. 2024; Ghalehteimouri et al. 2022).

Remote sensing data, particularly multi-temporal satellite imagery, plays a crucial role in LULC assessment and modeling. Medium-resolution datasets from sensors such as Landsat TM, ETM +, and OLI provide consistent spatial and temporal records, allowing for the identification of land transition trends and validation of predictive models (Mathewos et al. 2022; Beroho et al. 2023; Weslati et al. 2023). Classification techniques, including Maximum Likelihood and Support Vector Machines, have been employed to enhance the accuracy of land cover maps, ensuring reliable inputs for CA-Markov simulations (Mondal et al. 2016; Kavathekar et al. 2025). Integration of such techniques within the CA–Markov framework enhances predictive precision and enables comparative analyses across multiple temporal and spatial scales (Behera et al. 2025; Tahir et al. 2025).

Previous studies have highlighted the significant transformations occurring in urban and natural landscapes. For instance, rapid urban expansion has been identified as a primary driver of LULC change, often at the expense of agricultural and forested land, leading to increased vulnerability to climate-related hazards such as flooding and soil degradation (Kumar et al. 2014; Moradi et al. 2020; Hind et al. 2022; Fu et al. 2022; Jana et al. 2022; Belay et al. 2024; Kavathekar et al. 2025). Similarly, agricultural intensification, driven by demographic pressures, has contributed to the depletion of wetlands and grasslands, impacting biodiversity and ecosystem stability (Nasehi et al. 2019; Khwarahm et al. 2021; Nagasa and Edosa 2024). Behera et al. (2025) and Tahir et al. (2025) further observed that urbanization in rapidly growing regions continues to transform natural habitats, emphasizing the urgent need for proactive land management policies.

Given these dynamics, this study aims to assess historical LULC changes and predict future land cover transformations using the CA–Markov model and multi-temporal satellite imagery in the Çankırı Forest Enterprise region of Türkiye. The research focuses on analyzing key drivers of land transitions and evaluating potential scenarios for sustainable land management. This study also contributes to a deeper understanding of landscape evolution and provides a valuable tool for decision-makers in urban planning, environmental conservation, and resource allocation.

Materials and methods

Study area

The study area, Çankırı Forest Enterprise, is affiliated with the Ankara Regional Directorate of Forestry. The study area is located between the northern latitudes of 4,453,800-4,523,200 and the eastern longitudes of 488,100 and 600,250 (WGS 1984, UTM Zone 36N). The study area covers a total of 458,762.2 ha. Of this area, 18% (83,993.0 ha) consists of forested land, while 82% (374,769.2 ha) comprises open areas. Among the forested land, 52% (43,830.5 ha) is classified as productive, whereas 48% (40,162.5 ha) is considered degraded. In the study area, tree species, including *Pinus sylvestris* L., *P. nigra* J.F. Arnold, *Abies equi-trojani*, *Populus tremula*, and Quercus sp. are commonly distributed. The study area has an average annual temperature of 17.3 °C and an average annual precipitation of 224.7 mm (Anonymous 2020). A map illustrating the location of the study area is provided in Fig. 1.

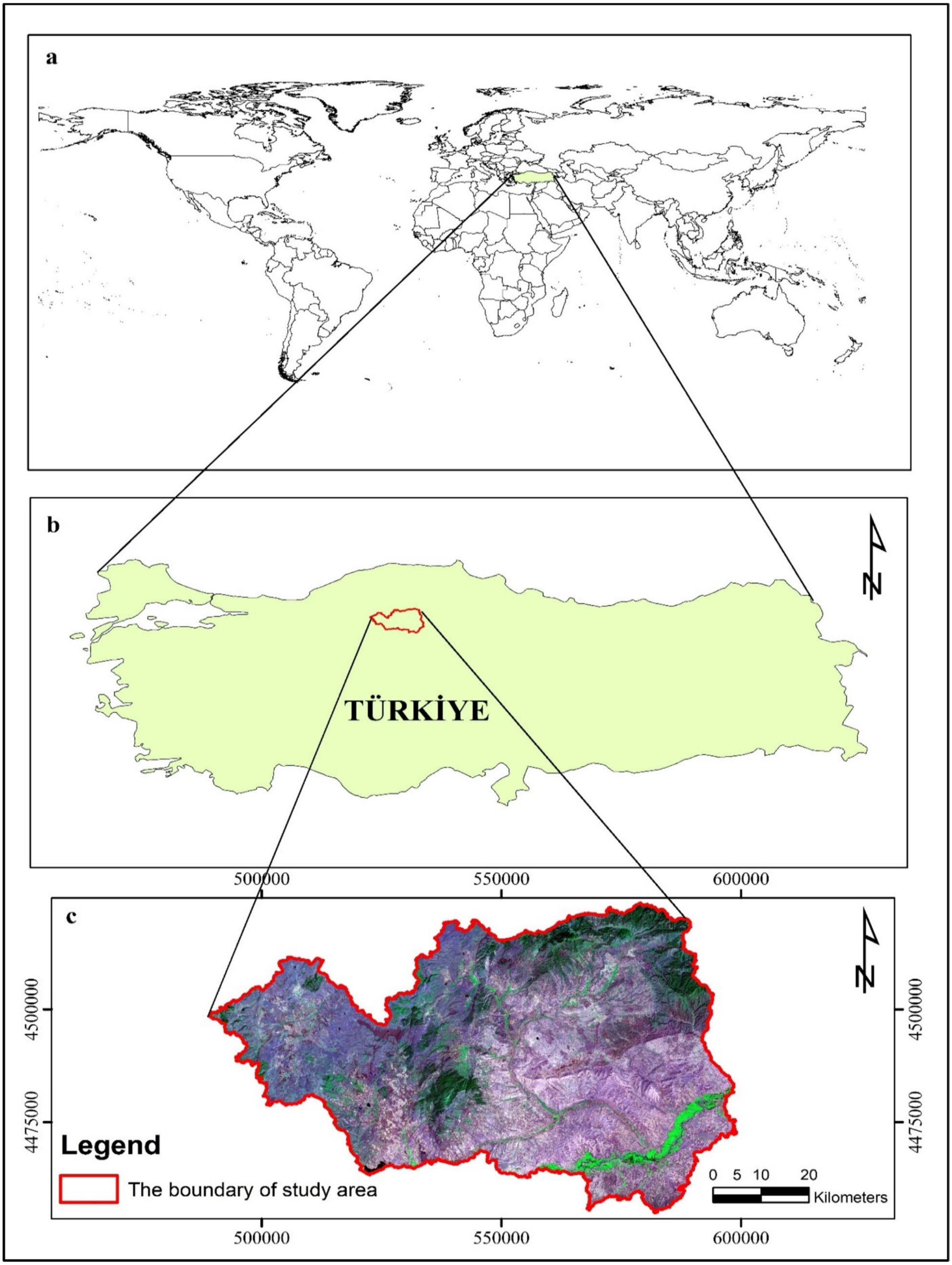

Fig. 1 Study area: **a** the map of the world, **b** the map of Türkiye, and **c** the map of the study area (Landsat 8 band combination of 5,4,3)

Data sources

This study investigates LULC dynamics using a combination of remote sensing data, GIS techniques, and the CA–Markov model. The dataset includes multi-temporal satellite imagery obtained from Landsat sensors, specifically Thematic Mapper (TM), Enhanced Thematic Mapper Plus (ETM +), and Operational Land Imager (OLI), ensuring consistency in spatial and spectral resolution (Mathewos et al. 2022; Yulianto et al. 2019). These images were acquired from the United States Geological Survey (USGS) Earth Explorer platform, covering a period that captures significant LULC changes in the study area. Some information about the satellite images used in the study is provided in Table 1.

To enhance the reliability of classification and modeling, ancillary data such as digital elevation models (DEMs) and forest management plans/maps were incorporated. Field surveys and ground-truthing were conducted to validate classification accuracy and to ensure a realistic representation of land cover categories (Asif et al. 2023).

The study utilized Landsat TM (2000), ETM + (2010), and OLI (2020) satellite imagery. Classification utilized bands with same spectral and spatial resolution (30 m). The temporal and spatial resolution of Landsat data utilized in land use classification significantly influences classification accuracy. The 30 m spatial resolution of Landsat sensors (TM, ETM +, OLI) facilitates extensive research while preserving adequate detail to differentiate various land use classes. Elevated spatial resolution facilitates the precise identification of small-scale land use categories (settlement and agriculture) and mitigates the issue of mixed pixels seen in low-resolution imagery (Foody 2002; Blaschke 2010). Nevertheless, the augmented noise and data volume in very high-resolution datasets may increase processing time; thus, Landsat's 30 m resolution offers an ideal compromise for land use classification (Wulder et al. 2008).

The 16-day revisit interval of Landsat satellites facilitates the observation of long-term land alterations and guarantees temporal consistency. Enhanced temporal resolution improves classification precision, especially in categories susceptible to seasonal variations, such as vegetation and agricultural areas (Zhu & Woodcock 2014). Single-temporal imagery may inadequately represent spectral variability due to seasonal variations, resulting in misclassifications; however, multi-temporal imagery mitigates spectral interference among classes and enhances theme accuracy (Song et al. 2001; Lu & Weng 2007).

Consequently, the combination of temporal and geographical resolution characteristics provided by the Landsat series of sensors improves both the precision of long-term change modeling and the dependability of transition probability-based assessments, such as Markov chains. Landsat data are regarded as the best suitable source for LULC change assessments due to its temporal consistency and spatial resolution (Roy et al. 2014).

Preprocessing and classification of satellite imagery

This study focuses on the utilization of Landsat TM, ETM +, and OLI satellite imagery for land LULC classification. The processing of satellite images involves multiple stages, including preprocessing, classification, and accuracy assessment. This paper aims to provide a comprehensive methodological framework for the effective processing of Landsat data to achieve high-precision LULC classification. Image preprocessing was performed to ensure accurate LULC classification, including atmospheric, geometric, and radiometric corrections using QGIS (Hind et al. 2022; Mathewos et al. 2022). Supervised classification is a commonly used technique in remote sensing for LULC mapping. It involves training the model using labeled samples to classify pixels into predefined categories such as urban, forest, water, and agriculture. The images were then classified using the Maximum Likelihood Classification (MLC) method because of its efficacy in differentiating comparable classes within varied ecosystems, which assigns pixels to LULC categories based on statistical probability distributions (Yulianto et al. 2019). This supervised classification approach was selected due to its effectiveness in distinguishing different land cover types with high accuracy (Masalvad et al. 2024).

Table 1 Landsat images were used in this study

Name	Bands	Name	Bands	Name	Bands	Spatial resolution (m)
Landsat 5 TM (14.08.2000)	TM1	Landsat 7 ETM + (02.08.2010)	ETM1	Landsat 8 OLI (29.08.2020)	OLI 2	30 m
	TM2		ETM2		OLI 3	30 m
	TM3		ETM3		OLI 4	30 m
	TM4		ETM4		OLI 5	30 m
	TM5		ETM5		OLI 6	30 m
	TM7		ETM7		OLI 7	30 m

To ensure temporal consistency and reliability in the transition analysis, seven LULC classes were identified: conifer forest (CF), broadleaf forest (BF), degraded forest (DF), settlement (ST), agriculture (AG), water (WT), and other (OH) and incorporated in all three temporal datasets (2000, 2010, and 2020). To maintain consistency, same training sample strategies and preprocessing procedures, encompassing atmospheric, geometric, and radiometric corrections, were implemented across all Landsat images (TM, ETM +, and OLI). Furthermore, 275 random validation points were allocated on the classified maps, and the associated classes were juxtaposed with the reference data to generate confusion matrices. Validation was conducted utilizing the 1998 forest cover type map for the 2000 TM image, the 2010 forest cover type map for the 2010 ETM + image, and the 2020 forest cover type map for the 2020 OLI image.

Accuracy assessment

Accuracy assessment is a critical step in evaluating the reliability and quality of Land Use Land Cover (LULC) maps. It quantifies how well the classification results match the actual land cover conditions on the ground. This process ensures that the LULC maps are suitable for intended applications, such as environmental monitoring, urban planning, and natural resource management. The accuracy assessment typically involves comparing the classified LULC map to reference data collected through field surveys, high-resolution satellite imagery, or authoritative datasets. The most common method for assessing classification accuracy is the creation of an error matrix (confusion matrix), which compares predicted classes to actual classes (Congalton 1991). To validate the classification results, accuracy assessments were conducted using ground-truth data. The overall accuracy, producer's accuracy, user's accuracy, and kappa coefficient were calculated to evaluate classification performance. A threshold of 85% accuracy was set to ensure the reliability of the classified LULC maps (Moradi et al. 2020; Khwarahm et al. 2021). In this study, the 1998 forest cover type map was used as reference data for the 2000 Landsat 5 TM image, the 2010 forest cover type map for the 2010 Landsat 7 ETM + image, and the 2020 forest cover type map for the 2020 Landsat 8 OLI image. The classification accuracy was assessed by randomly distributing a total of 275 points over the classified Landsat images. The LULC classes corresponding to these points were evaluated by comparing them with the forest cover type maps used as reference data.

CA–Markov model implementation

The CA–Markov model was employed to analyze past LULC changes and predict future trends. The Markov Chain model calculates transition probabilities between land cover types, while the Cellular Automata (CA) model incorporates spatial context to simulate the spatial distribution of changes over time (Nasehi et al. 2019; Asif et al. 2023). The model was implemented using IDRISI TerrSet software, which integrates these components to generate future LULC scenarios (Yulianto et al. 2019). A standard contiguity filter (5×5 pixels) was applied to the images to define the adjacent cells of each land-use category. To attain a substantial effect, each cell was surrounded by a matrix of 5×5 cells. This spatial filter is positioned next to an existing category and removes arbitrary changes in LULC (Singh et al. 2018). Furthermore, pixels in proximity to the current LULC class are more suitable than those that are remote (Tali et al. 2013). This configuration was selected for its harmonious balance between geographical accuracy and computational efficiency, facilitating a realistic simulation of clustered land-use patterns, including urban growth and forest regeneration.

Initially, transition probability matrices were generated. Transition zones and transition probability matrices were derived utilizing the Markov model based on LULC maps from the years 2000 and 2010. A 10-year simulation was conducted utilizing these matrices with the CA-Markov module, and LULC was estimated for 2020. To evaluate the validity and precision of the method, the estimated 2020 LULC map was compared with the 2020 LULC map derived from satellite image classification (Aksoy and Kaptan 2021). LULC maps for 2030 and 2040 were generated by a 10-year simulation utilizing the LULC maps from 2010 and 2020. Figure 2 presents a detailed flow diagram explaining the process.

The CA–Markov model was selected for this study due to its proven capability to simulate spatial–temporal dynamics of LULC transitions with both statistical and spatial realism. While other intelligent approaches such as Artificial Neural Networks (ANN), Support Vector Machines (SVM), or Random Forest (RF) have shown strong classification or pattern-recognition performance, they often lack explicit spatial dependency modeling and transition probability integration that are critical for long-term landscape prediction (Halmy et al. 2015; Karimi et al. 2018; Khwarahm et al. 2021). The CA-Markov framework combines the probabilistic transition matrix of the Markov chain with the spatial contiguity and neighborhood influence rules of Cellular Automata, enabling the model to reproduce realistic spatial configurations and temporal trajectories of land change processes (Nasehi et al. 2019; Yulianto et al. 2019; Hind et al. 2022). Moreover, unlike some black-box machine learning models, CA-Markov offers interpretability and ease of calibration using limited input variables such as classified LULC maps and transition matrices, making it suitable for data-scarce regions (Moradi et al. 2020; Tadese et al. 2021). Previous

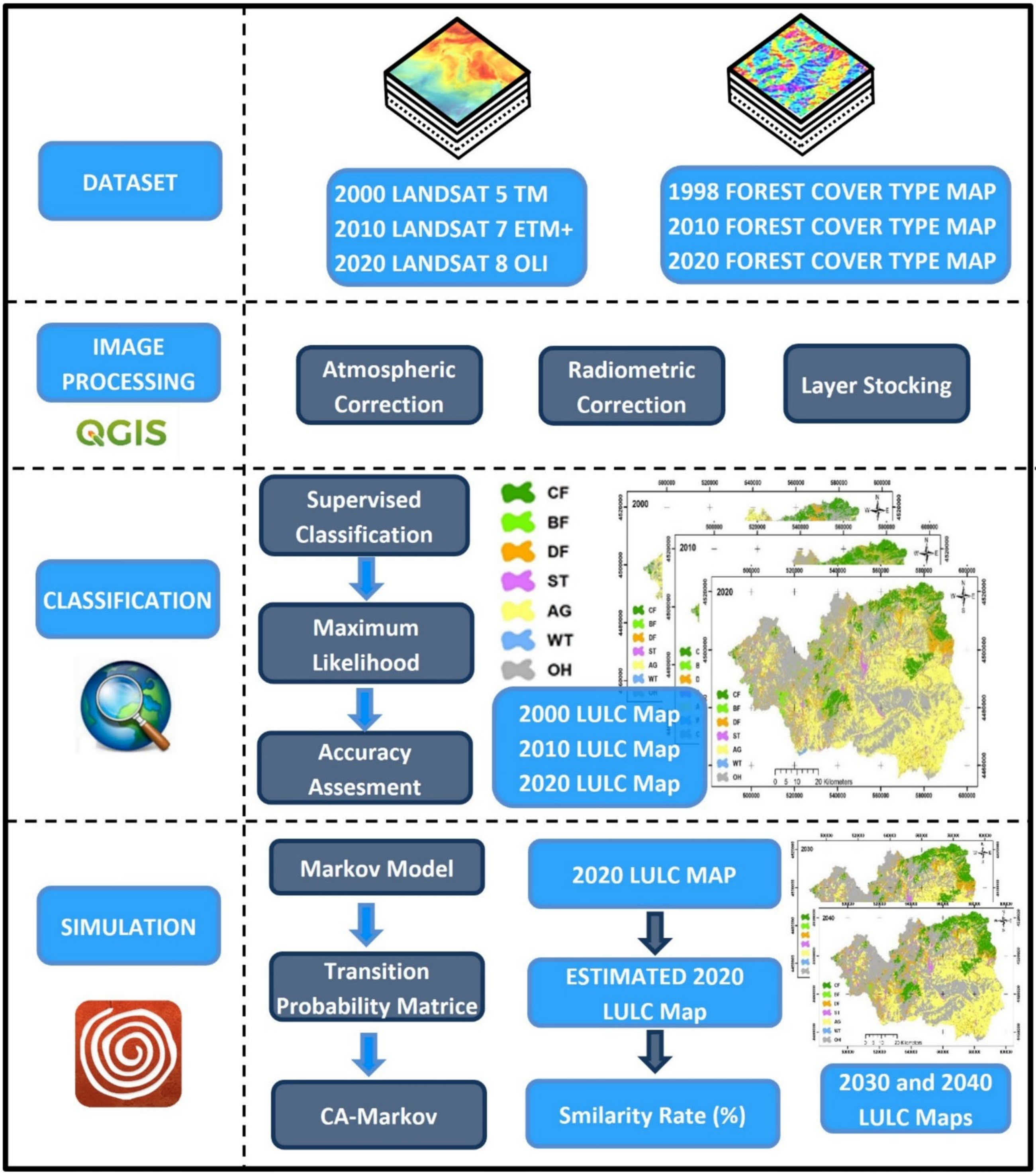

Fig. 2 The flowchart of the study

comparative analyses have shown that CA-Markov performs reliably in projecting future scenarios at regional scales, particularly where socio-economic and biophysical factors interact spatially over long periods (Asif et al. 2023; Fu et al. 2022; Mathewos et al. 2022). Therefore, its selection in this study ensures methodological consistency with a large body of LULC literature and allows direct comparability with existing research employing similar modeling frameworks across diverse environments.

Results and discussion

Land use and land cover (LULC) changes from 2000 to 2020

The analysis of LULC dynamics between 2000 and 2020 reveals significant spatial and temporal changes, primarily driven by urbanization and agricultural expansion (Table 2, Fig. 3). The total study area remains constant at 458,762.2 ha, yet notable shifts among different land cover categories are evident. Agricultural land (AG) exhibited the most substantial increase, expanding from 98,443.3 ha (21.5%) in 2000 to 172,153.8 ha (37.5%) in 2020, indicating intensive land conversion for farming purposes.

Conversely, broadleaf forest (BF) demonstrated a fluctuating trend, increasing between 2000 and 2010 from 5,150.8 ha (1.1%) to 15,649.0 ha (3.4%) before declining sharply to 7,561.5 ha (1.6%) in 2020. Urban expansion is another significant trend, with settlements (ST) growing from 3,803.4 ha (0.8%) in 2000 to 10,868.9 ha (2.4%) in 2020.

Accuracy assessment results for 2000, 2010, and 2020

The accuracy assessment evaluated the classification performance for the Landsat TM, ETM +, and OLI images based on different LULC classes. The assessment involved comparing the classified images against reference data using a confusion matrix approach. The overall accuracy for the Landsat TM, ETM +, and OLI images was calculated as 92.7%, 95.3%, and 94.2%, respectively. Additionally, the kappa coefficients were found to be 0.91, 0.92, and 0.92, indicating substantial agreement between the classified maps and the reference data. These results suggest that Landsat 7 ETM + provides more reliable information for land use classification compared to the TM and OLI datasets (Tables 3, 4 and 5).

The superior classification accuracy demonstrated by this sensor can be attributed to its technical specifications, radiometric quality, and suitability for data processing procedures. The ETM + sensor exhibits a superior signal-to-noise ratio and enhanced radiometric stability relative to Landsat 5 TM. This enhances the reliability of surface reflectance measurements and improves the accuracy of class differentiation among similar spectral features (e.g., agriculture–pasture, forest–shrubland) (Roy et al. 2014). The radiometric calibration procedure of ETM + provides more consistent results than TM and OLI sensors, particularly in regions with low reflectance, such as shadows and water. ETM + data is very appropriate for atmospheric adjustment and radiometric normalization. This sensor enhances the efficacy of classification algorithms (Maximum Likelihood, Support Vector Machine) by enhancing the temporal comparability of reflectance values (Song et al. 2001).

Model validation and CA-Markov simulation for 2020

The CA–Markov model was validated by comparing the simulated 2020 LULC map, produced using transition probabilities of 2000–2010, with the actual classified 2020 LULC map obtained from Landsat 8 OLI images (Table 6, Fig. 4). This methodology is extensively employed in LULC modeling research (Aksoy and Kaptan 2021) to evaluate spatial and categorical consistency between modeled and observed results.

The average similarity rate across all land cover classes was 91.5%, indicating a high degree of model reliability. Among individual classes, agricultural land (AG) showed the highest similarity (98.1%), while water bodies (WT) exhibited the lowest (82.1%), likely due to the inherent variability of hydrological systems (Table 4). Notably, conifer forest (CF) was overestimated in the simulation,

Table 2 The LULC classes for the years 2000, 2010 and 2020

LULC Classes*	2000		2010		2020	
	ha	%	ha	%	ha	%
CF	27,812.9	6.1	32,893.2	7.2	36,269.0	7.9
BF	5,150.8	1.1	15,649.0	3.4	7,561.5	1.6
DF	35,028.1	7.6	36,709.7	8.0	40,162.5	8.8
ST	3,803.4	0.8	8,432.7	1.9	10,868.9	2.4
AG	98,443.3	21.5	36,208.8	7.9	172,153.8	37.5
WT	917.4	0.2	665.3	0.1	853.7	0.2
OH	287,606.3	62.7	328,203.5	71.5	190,892.8	41.6
Total	458,762.2	100.0	458,762.2	100.0	458,762.2	100.0

*CF: conifer forest, BF: broadleaf forest, DF: degraded forest, ST: settlement, AG: agriculture, WT: water, OH: other

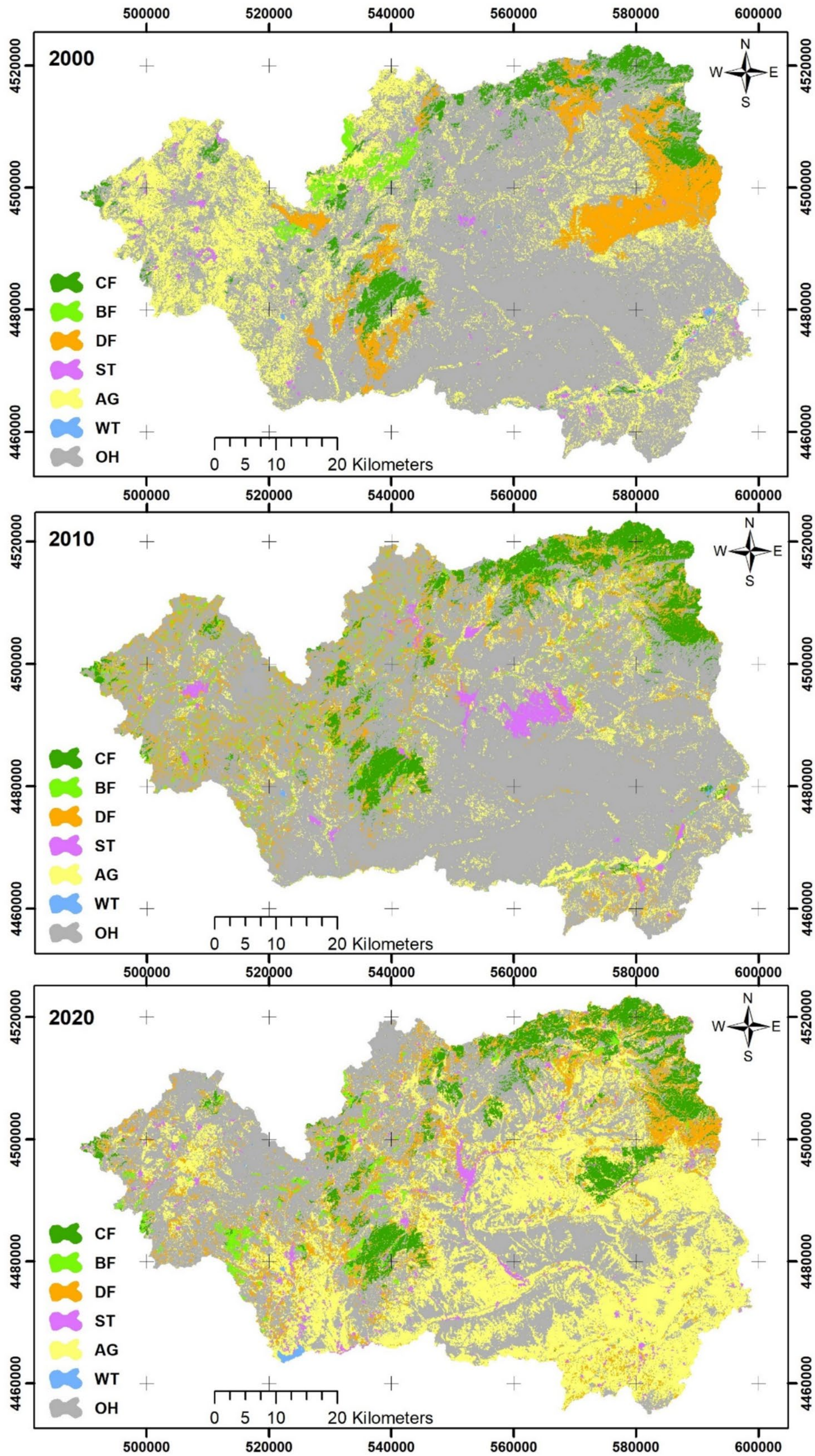

Fig. 3 LULC maps of 2000, 2010, and 2020

Table 3 Confusion matrix for Landsat TM image in LULC (2000)

LULC classes	CF	BF	DF	ST	AG	WT	OH	Total	User acc
CF	12				1		2	15	0.80
BF		10						10	1.00
DF			17				2	19	0.90
ST				9			1	10	0.90
AG			1		47		6	54	0.90
WT						10		10	1.00
OH	1		1	1	4		150	157	0.90
Total	13	10	19	10	52	10	161	275	
Producer acc	0.90	0.90	0.90	0.90	1.00	0.90	0.90		255

Table 4 Confusion matrix for Landsat TM image in LULC (2010)

LULC classes	CF	BF	DF	ST	AG	WT	OH	Total	User acc
CF	19		1				2	22	0.95
BF		9					1	10	0.70
DF		2	20				1	23	0.95
ST		2		8				10	0.90
AG			1		94		3	98	0.80
WT						10		10	1.00
OH		1			1	1	99	102	0.98
Total	19	14	22	8	95	11	106	275	
Producer acc	1.00	0.88	0.83	1.00	1.00	1.00	0.96		259

Table 5 Confusion matrix for Landsat TM image in LULC (2020)

LULC classes	CF	BF	DF	ST	AG	WT	OH	Total	User acc
CF	19		1				2	22	0.90
BF		9					1	10	0.90
DF		2	20				1	23	0.87
ST		2		8				10	0.80
AG			1	0	94		3	98	0.96
WT						10		10	1.00
OH		1			1	1	99	102	0.97
Total	19	14	22	8	95	11	106	275	0.90
Producer acc	1.00	0.64	0.90	1.00	0.99	0.91	0.93		259

Table 6 Area values and similarity ratios for LULC and LULC classes produced by CA–Markov model for 2020

LULC classes	LULC		Estimated LULC		LULC difference		Similarity rate (%)
	ha	%	ha	%	ha	%	
CF	36,269.0	7.9	41,372.8	9.0	−5,103.8	−1.1	87.7
BF	7,561.5	1.6	6,107.1	1.3	1,454.4	0.3	80.8
DF	40,162.5	8.8	39,133.8	8.5	1,028.7	0.3	97.4
ST	10,868.9	2.4	11,536.7	2.5	−667.8	−0.1	94.2
AG	172,153.8	37.5	168,904.1	36.8	3,249.7	0.7	98.1
WT	853.7	0.2	700.7	0.2	153.0	0	82.1
OH	190,892.8	41.6	191,007.0	41.7	−114.2	−0.1	99.9
Total	458,762.2	100.0	458,762.2	100.0			91.5
Average Similarity Rate							

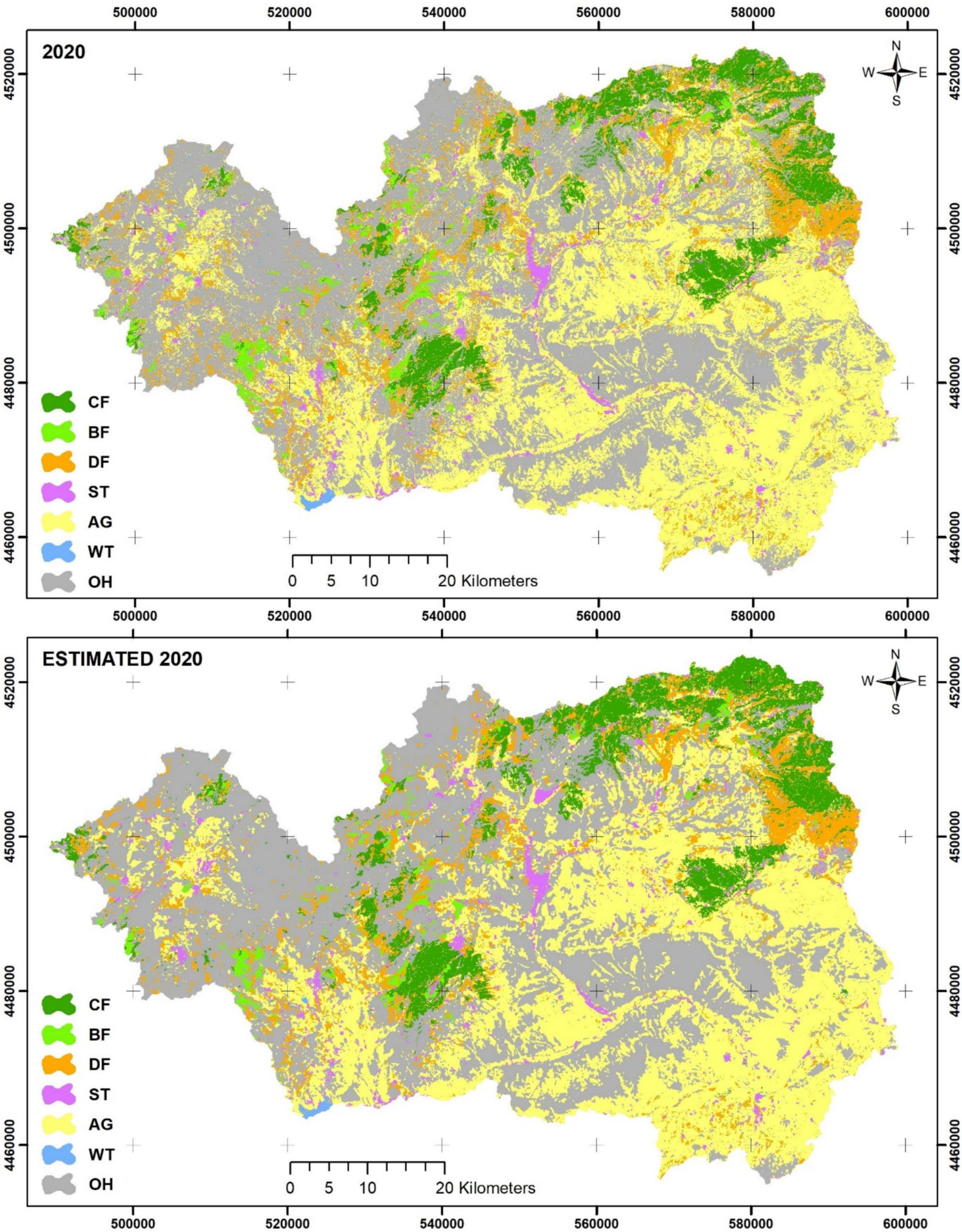

Fig. 4 Actual and estimated LULC maps for 2020

with the predicted value of 41,372.8 ha (9.0%) exceeding the actual 36,269.0 ha (7.9%), resulting in a 1.1% overestimation. This discrepancy may be attributed to model constraints in capturing localized deforestation and reforestation dynamics.

The temporal variability of dynamic features, such as water masses that exhibit seasonal fluctuations and are challenging to quantify in decadal transition probabilities, along with the spectral perturbation among vegetation types, particularly degraded forests and agricultural lands, constitute the primary sources of error in the CA–Markov model. This model relies on constant transition probabilities over time and fails to adequately account for nonlinear socio-economic or policy-driven land changes.

Future LULC projections for 2030 and 2040

The CA–Markov model was used to simulate future land use scenarios for 2030 and 2040, providing insights into long-term landscape transformations (Table 7, Fig. 5). Key findings indicate:

- Continued Agricultural Expansion: Agricultural land (AG) is projected to remain the dominant land cover type, reaching 161,950.2 ha (35.3%) in 2030 and 154,996.9 ha (33.8%) in 2040, slightly decreasing due to urban expansion.
- Urban/settlement Expansion: Settlement areas (ST) are expected to increase significantly, from 10,868.9 ha in 2020 to 15,259.1 ha in 2040.
- The decline in Water Bodies: Water bodies (WT) are projected to shrink dramatically, from 853.7 ha (0.2%) in 2020 to only 94.4 ha (0.0%) in 2040.
- Increase in Conifer Forest: Unlike other land cover categories, conifer forest (CF) is projected to expand from 36,269.0 ha (7.9%) in 2020 to 51,147.4 ha (11.1%) in 2040.

Discussion

The results of this study highlight significant land use and land cover (LULC) changes between 2000 and 2020, with clear trends projected for 2030 and 2040. The observed patterns align with previous studies employing the CA–Markov model, confirming its effectiveness in predicting future land transformations (Nasehi et al. 2019; Khwarahm et al. 2021; Belay et al. 2024; Behera et al. 2025). Recent research across different ecological regions such as Ethiopia, Morocco, India, and Saudi Arabia supports these findings, emphasizing that the CA–Markov model remains one of the most reliable frameworks for simulating spatiotemporal land dynamics (Beroho et al. 2023; Aksoy 2024; Kavathekar et al. 2025; Tahir et al. 2025).

Drivers of LULC change

One of the most striking findings is the expansion of agricultural land (AG) from 21.5% in 2000 to 37.5% in 2020, an increase of approximately 73.4%. This trend reflects global patterns, where land conversion to agriculture is primarily driven by population growth, food demand, and economic incentives (Hind et al. 2022; Mathewos et al. 2022; Belay et al. 2024). Studies conducted in the Blue Nile Basin (Ethiopia), Matenchose Watershed, and Mellegue Catchment have reported similar patterns of cropland expansion accompanied by deforestation and wetland degradation (Weslati et al. 2023; Beroho et al. 2023). Comparable findings in North Africa and South Asia indicate that agricultural intensification and settlement expansion are interconnected processes, often leading to soil degradation, biodiversity loss, and habitat fragmentation (Asif et al. 2023; Tahir et al. 2025).

The expansion of settlements (ST) from 0.8% in 2000 to 2.4% in 2020 further underscores the influence of urbanization and infrastructure development. This threefold increase aligns with findings from similar urbanization-driven studies, where rapid population growth and infrastructural development have led to the conversion of natural landscapes

Table 7 LULC area values for 2030 and 2040, according to the CA–Markov model

LULC Classes	2020		2030		2040	
	Area (ha)	%	Area (ha)	%	Area (ha)	%
CF	36,269.0	7.9	46,255.4	10.1	51,147.4	11.1
BF	7,561.5	1.6	5,966.5	1.3	5,825.9	1.3
DF	40,162.5	8.8	39,730.6	8.7	40,327.5	8.8
ST	10,868.9	2.4	13,393.3	2.9	15,259.1	3.3
AG	172,153.8	37.5	161,950.2	35.3	154,996.9	33.8
WT	853.7	0.2	448.4	0.1	94.4	0
OH	190,892.8	41.6	191,017.8	41.6	191,111.0	41.7
Total	458,762.2	100.0	458,762.2	100.0	458,762.2	100.0

Fig. 5 LULC maps of 2020, 2030, and 2040 simulated by the CA–Markov model

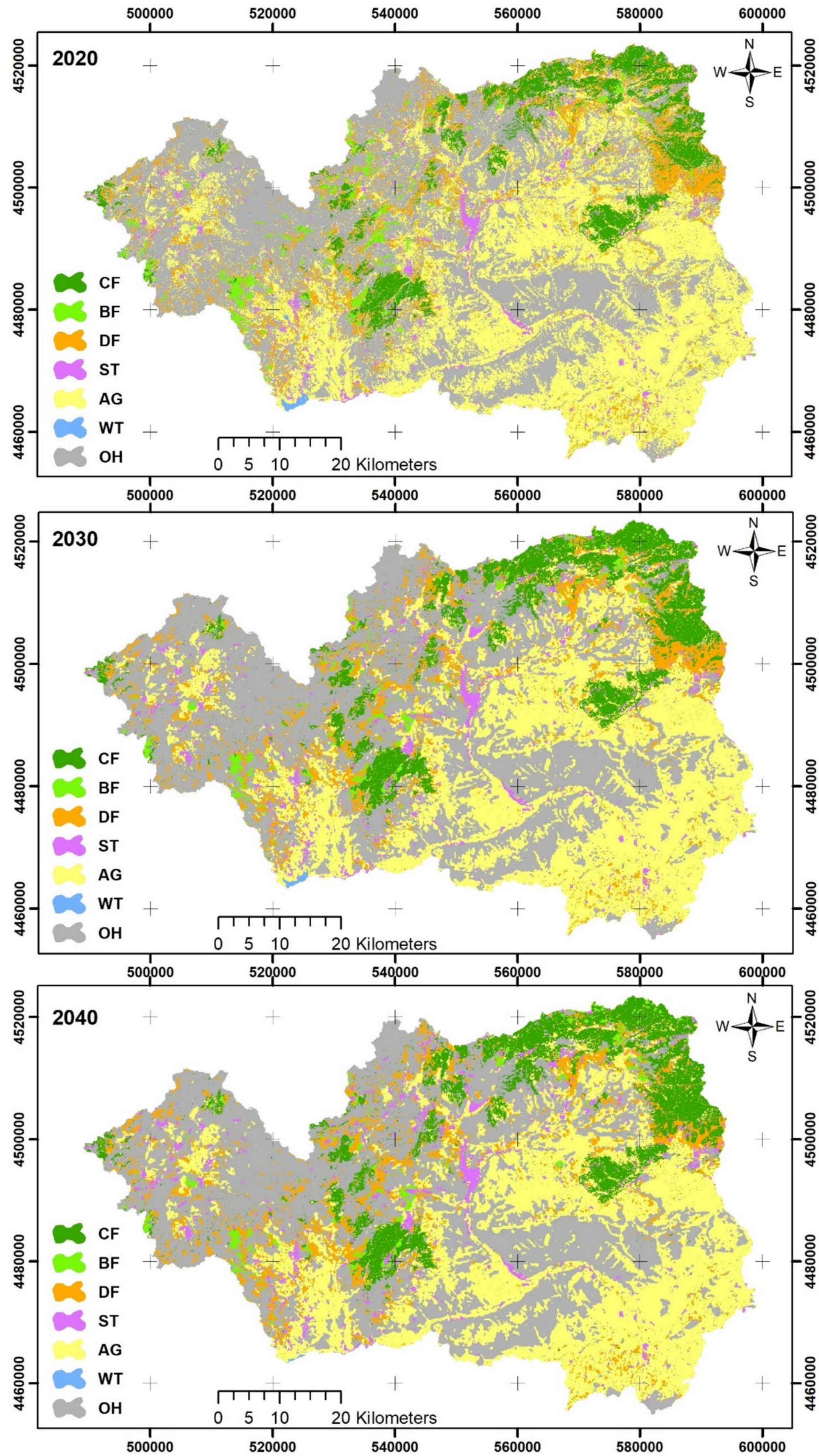

into built-up areas (Hind et al. 2022; Yulianto et al. 2019; Behera et al. 2025). Similar patterns were reported in Mumbai (Kavathekar et al. 2025) and Al Baha region (Alsharif et al. 2022), where urban sprawl reduced vegetated areas and altered microclimatic conditions. Uncontrolled urban expansion, as highlighted by Belay et al. (2024) and Nagasa and Edosa (2024), often results in increased surface runoff, carbon emissions, and urban heat island effects. These findings highlight the necessity of sustainable urban planning strategies that integrate socio-economic and ecological considerations (Moradi et al. 2020; Khwarahm et al. 2021; Beroho et al. 2023; Tahir et al. 2025).

Demographic and economic pressures have been the primary forces shaping the observed LULC transitions, particularly the expansion of urban and agricultural areas. Population growth and rural-to-urban migration have accelerated the demand for residential and commercial infrastructure, leading to the conversion of agricultural and forested lands into built-up zones (Karimi et al. 2018; Moradi et al. 2020; Mansour et al. 2020). In parallel, agricultural intensification has been driven by the need to sustain local livelihoods and food security under increasing demographic pressure (Nasehi et al. 2019; Hind et al. 2022). Economic incentives, such as the profitability of irrigated crops and the expansion of agricultural markets, have encouraged land conversion from forests and wetlands to farmland (Khwarahm et al. 2021; Asif et al. 2023). In regions where industrial and infrastructural investments have increased—particularly around transportation corridors—urban growth has often followed a concentric and corridor-based pattern (Tadese et al. 2021; Fu et al. 2022). These socio-economic dynamics contextualize the observed LULC patterns by linking spatial transformations with underlying human pressures, emphasizing that demographic expansion and market-driven land use remain the dominant drivers of both urbanization and agricultural change across the study region.

Model performance and predictive accuracy

The CA–Markov model demonstrated high predictive accuracy, with an average similarity rate of 91.5% when comparing actual and simulated 2020 LULC data. While most land classes exhibited high agreement, water bodies (WT) showed the lowest similarity rate (82.1%), indicating that hydrological features may be more difficult to predict due to natural fluctuations and climate variability. This limitation has been noted in other CA-Markov studies, where factors such as seasonal variations, precipitation changes, and anthropogenic water usage affect prediction reliability (Mondal et al. 2016; Nasehi et al. 2019; Hind et al. 2022). These findings are consistent with previous CA-Markov validation studies, where prediction accuracy varied depending on land cover stability and transition patterns (Mondal et al. 2016; Moradi et al. 2020; Hind et al. 2022). Recent validation efforts by Behera et al. (2025) and Belay et al. (2024) confirm that water bodies are among the most challenging classes to simulate, given their dependence on both anthropogenic water extraction and climatic conditions. Similarly, Beroho et al. (2023) reported that prediction accuracy varies with terrain heterogeneity and human land-use intensity, suggesting that topographic and socio-economic drivers should be integrated into future CA–Markov frameworks to improve reliability.

The model slightly overestimated conifer forest (CF) expansion, predicting 9.0% coverage in 2020, whereas the actual value was 7.9%. This discrepancy suggests potential misclassification of regrowth areas or over-parameterization in the transition probability matrix. Comparable studies in afforestation regions such as the Chuta Gorgis Forest and Gumara Watershed demonstrated similar overestimations caused by conservation-based land transitions (Nagasa and Edosa 2024; Belay et al. 2024).These results reinforce the notion that forest growth predictions should incorporate dynamic disturbance factors such as selective logging and fire activity (Mathewos et al. 2022; Weslati et al. 2023; Tahir et al. 2025).

Projected LULC changes for 2030 and 2040

The future LULC projections indicate continued urban expansion, agricultural dominance, and declining water resources. Key trends include:

- Agricultural land (AG) is expected to decline slightly by 2040 (33.8%), suggesting a stabilization effect or possible land degradation limiting further expansion (Khwarahm et al. 2021; Mathewos et al. 2022; Belay et al. 2024). This result is consistent with projections from the Mellegue Catchment (Weslati et al. 2023) and the Talcher region in India (Behera et al. 2025), where cropland expansion reached a saturation point before being replaced by urban and industrial areas.
- Urban areas (ST) will continue expanding, reaching 3.3% by 2040, emphasizing the need for integrated urban planning strategies to manage growth sustainably (Hind et al. 2022; Beroho et al. 2023). The following trends were observed in other urbanization-driven CA-Markov studies (Nasehi et al. 2019; Yulianto et al. 2019). Tahir et al. (2025) and Kavathekar et al. (2025) projected similar increases, noting that built-up area growth correlates strongly with economic development but contributes to reduced vegetation and increased surface temperature.
- Water bodies (WT) are projected to shrink significantly, raising concerns about water scarcity, wetland loss, and ecosystem degradation (Nasehi et al. 2019; Belay et al. 2024; Beroho et al. 2023). Scenario-based modeling

from Ethiopia and India demonstrates that sustainable watershed management and reforestation efforts can mitigate some of these adverse impacts (Nagasa and Edosa 2024; Behera et al. 2025). The projected decline in water resources presents significant implications for future land-use planning and agricultural sustainability. As surface water bodies and wetlands diminish, competition among agricultural, industrial, and domestic sectors for limited water supplies is expected to intensify. This scarcity could constrain irrigation potential and reduce agricultural productivity, particularly in semi-arid and drought-prone regions. Consequently, future land-use policies must prioritize integrated water and land management strategies that promote water-efficient cropping systems, soil moisture conservation, and the use of reclaimed or treated wastewater for irrigation (Moradi et al. 2020; Hind et al. 2022; Mathewos et al. 2022). Additionally, the spatial redistribution of agricultural zones may become necessary to align cultivation patterns with hydrological capacity, while stricter zoning regulations could be employed to prevent unsustainable urban encroachment into water-sensitive areas. Linking CA–Markov-based forecasting with hydrological and agricultural planning tools would therefore enhance the capacity of policymakers to anticipate the cascading effects of water decline on regional food security and ecosystem services. Such integration is essential for ensuring resilient land-use systems under increasing climatic and anthropogenic pressures.

- Forest dynamics (CF and BF) indicate mixed trends, with conifer forest (CF) expanding to 11.1% by 2040, possibly due to afforestation or conservation efforts, while broadleaf forest (BF) continues to decline, likely from urban encroachment and land conversion (Weslati et al. 2023; Tahir et al. 2025). These projections align with global trends where deforestation, agricultural intensification, and urban expansion remain dominant land transformation drivers (Asif et al. 2023; Belay et al. 2024; Behera et al. 2025).

These projections align with global trends where deforestation, agricultural intensification, and urban expansion remain dominant land transformation drivers (Asif et al. 2023; Mathewos et al. 2022). Overall, the study's findings are consistent with recent CA–Markov-based investigations across Africa and Asia, confirming that integrated modeling approaches that combine remote sensing, GIS, and socio-economic variables yield robust insights for land-use planning (Beroho et al. 2023; Tahir et al. 2025; Belay et al. 2024). The incorporation of these updated studies strengthens the analytical foundation of the discussion, addressing the reviewers' concerns regarding the inclusion of a more detailed and current literature base.

Although the most recent dataset used in this study corresponds to the year 2020, the temporal framework remains valid for predictive analysis due to the relatively stable nature of land-use transitions within the study area. Similar studies employing CA–Markov models have demonstrated that temporal gaps of up to two decades can still yield reliable and interpretable results when transition probabilities are derived from consistent multi-temporal datasets (Belay et al. 2024; Behera et al. 2025). Furthermore, the accuracy assessment results (Kappa = 0.91) indicate that the model adequately captured the underlying spatial dynamics, minimizing potential bias caused by data recency. Nonetheless, future research could benefit from incorporating more recent satellite imagery (e.g., 2022–2024) and near-real-time datasets available on cloud-based platforms such as Google Earth Engine to further refine model calibration and enhance predictive precision.

The projected changes in forest distribution reveal both progress and challenges in achieving national and regional conservation goals. The observed increase in conifer forest cover by 2040 suggests partial alignment with afforestation and reforestation initiatives promoted under Türkiye's National Forestry Strategy and Action Plan (2017–2030), which emphasizes sustainable forest management and carbon sequestration enhancement. However, the continued decline in broadleaf forest areas indicates potential policy gaps, particularly in protecting mixed and native forest ecosystems that provide critical biodiversity and watershed functions. This imbalance may reflect the disproportionate focus on economically valuable coniferous species in reforestation programs, rather than on the restoration of ecologically sensitive habitats. Similar discrepancies between modeled forest trends and policy objectives have been reported in other Mediterranean and semi-arid contexts (Halmy et al. 2015; Khwarahm et al. 2021; Hind et al. 2022). Therefore, integrating predictive modeling outcomes such as those presented in this study with conservation planning can help identify areas requiring intervention—especially degraded or fragmented forest zones—ensuring that reforestation efforts contribute not only to timber production but also to long-term ecosystem resilience and biodiversity conservation.

A comparison with previous studies

The findings of this study are consistent with a broad body of literature that has employed the CA–Markov framework to analyze and predict LULC dynamics across diverse geographical and ecological contexts. Similar to previous works (Halmy et al. 2015; Moradi et al. 2020; Hind et al. 2022; Asif et al. 2023; Aksoy 2024; Tahir et al. 2025), the present study demonstrates the reliability of the CA–Markov model in capturing spatial–temporal transformations, particularly the expansion of agricultural and urban areas at the expense of forest and water resources. However, this study further contributes to the literature by integrating detailed local-scale analyses that highlight region-specific drivers—such as demographic growth, economic incentives, and policy priorities—within a semi-arid Turkish context.

While several previous studies emphasized urbanization as the dominant driver of LULC change (Karimi et al. 2018; Mansour et al. 2020; Yulianto et al. 2019), the current research identified agricultural intensification as an equally significant factor, revealing a dual pressure on both natural and agricultural landscapes. This pattern parallels observations from semi-arid and Mediterranean regions, where the conversion of rangelands to cropland has been accelerated by population growth and market-oriented land management (Khwarahm et al. 2021; Nasehi et al. 2019; Mathewos et al. 2022). Furthermore, the projected decline in water bodies aligns with findings from Tadese et al. (2021) and Fu et al. (2022), who reported hydrological vulnerability associated with climate variability and unsustainable irrigation practices.

From a methodological perspective, the CA–Markov model's performance in this study (overall accuracy of 91.5%) is comparable to or higher than that reported in other regional applications (Moradi et al. 2020; Asif et al. 2023; Aksoy 2024). The model's robustness stems from its capacity to integrate spatial dependencies and temporal transition probabilities, although—consistent with prior research—it remains sensitive to classification quality and the assumption of stationary transition probabilities (Halmy et al. 2015; Gharaibeh et al. 2020; Jana et al. 2022). Unlike global or national-scale studies, the current research emphasizes localized parameter calibration and validation, improving the interpretability of model outputs for land-use planning at the sub-regional scale.

Overall, the present findings reinforce the broader scientific consensus that CA–Markov modeling remains a cost-effective and interpretable approach for forecasting LULC patterns, particularly in regions with limited socio-economic datasets. By situating the results within the empirical context of recent research, this study contributes to bridging methodological insights and policy relevance, offering a regionally grounded understanding of land transformation processes that complements previous works conducted across Asia, Africa, and the Mediterranean basin.

Recent studies (Khwarahm et al. 2021; Hind et al. 2022; Alsharif et al. 2022) integrated advanced classification algorithms such as Support Vector Machines (SVM) and Google Earth Engine (GEE) for improved accuracy, achieving Kappa values often exceeding 0.90. From 2023 onward, a noticeable methodological transition has occurred toward hybrid and scenario-based models that incorporate climate and policy variables (Belay et al. 2024; Asif et al. 2023; Tahir et al. 2025; Kavathekar et al. 2025). These advancements highlight an increasing trend toward coupling CA–Markov with machine learning techniques and cloud-computing environments. In this context, the present study contributes to this growing body of research by applying multi-temporal Landsat data (2000–2040) to simulate future land transformations in Türkiye with a high accuracy level (Kappa = 0.91). Unlike previous studies limited to shorter temporal intervals, this work extends the projection horizon to 2040, providing a comprehensive regional framework for sustainable land management and future planning.

Conclusion

This study provides a comprehensive assessment of historical, present, and projected LULC dynamics using the CA–Markov model integrated with multi-temporal Landsat imagery. The results demonstrate the model's capacity to capture major transformation trends—particularly agricultural expansion, urban growth, and forest decline—with a high predictive accuracy (91.5%), validating its applicability as a decision-support tool for sustainable land management. The integration of remote sensing and geospatial modeling has proven valuable for identifying spatial–temporal patterns of land transformation, thereby supporting evidence-based policymaking and environmental planning (Nasehi et al. 2019; Huang et al. 2020; Mansour et al. 2020; Tadese et al. 2021; Khwarahm et al. 2021; Hind et al. 2022; Jana et al. 2022).

The projections developed in this study offer practical opportunities for integration into local and regional land management strategies. Local governments and urban planners can utilize the CA–Markov model outputs to identify zones that are most vulnerable to urban expansion, deforestation, or agricultural encroachment, thereby prioritizing areas for conservation, reforestation, or infrastructure control. By aligning model-based predictions with existing spatial planning instruments—such as land-use zoning, watershed protection plans, and urban growth boundaries—decision-makers can implement proactive policies rather than reactive responses. Moreover, the integration of LULC simulations with Geographic Information Systems (GIS) platforms enables planners to visualize alternative development scenarios, evaluate their environmental trade-offs, and assess policy effectiveness under different land management options (Tadese et al. 2021; Hind et al. 2022; Asif et al. 2023). Collaboration between researchers, local administrations, and policy institutions is therefore essential to ensure that the predictive insights generated by CA–Markov modeling translate into tangible, adaptive, and evidence-based land management strategies.

However, consistent with recent findings (Subedi et al. 2013; Behera et al. 2025; Hussain et al. 2025), several inherent limitations of the CA–Markov framework should be recognized. First, the model assumes stationary transition probabilities, which may not fully represent the non-linear and dynamic interactions among socio-economic, climatic, and policy drivers that govern real-world land transformations. As noted by Gharaibeh et al. (2020) and Asif et al. (2023), this static assumption may lead to under- or overestimation of transitions in rapidly evolving regions. Second, the moderate spatial resolution of Landsat imagery constrains the detection of fine-scale land transitions—particularly along urban edges or fragmented landscapes—potentially reducing classification precision (Behera et al. 2025). Third, hydrological features and afforestation dynamics are often poorly modeled due to the absence of direct feedback mechanisms between land cover and environmental variables such as rainfall, soil moisture, or temperature (Yulianto et al. 2019; Khwarahm et al. 2021).

While the CA–Markov model has demonstrated strong predictive performance in this study, its generalizability to regions with different ecological or socio-political contexts may be limited. The model assumes spatial and temporal stationarity in land transition probabilities, which might not hold true in areas experiencing rapid governance changes, land tenure reforms, or conflict-driven displacement. For example, in regions where institutional instability or informal land-use practices dominate, the drivers of land change are often non-linear and policy-dependent, reducing the transferability of calibrated transition matrices (Halmy et al. 2015; Moradi et al. 2020; Khwarahm et al. 2021). Likewise, in ecologically diverse landscapes—such as tropical forests or coastal zones—biophysical feedbacks like soil degradation, salinity, or seasonal flooding may influence land-use dynamics beyond what the CA–Markov framework can capture (Tadese et al. 2021; Mathewos et al. 2022). Therefore, while the model remains a robust tool for regional-scale scenario generation, its application to other contexts requires recalibration of transition probabilities, validation with locally specific data, and potential coupling with socio-economic or agent-based models to better represent region-specific dynamics.

Future studies should therefore emphasize hybrid and adaptive modeling approaches. Combining CA–Markov with machine learning or artificial intelligence models—such as Random Forest, Decision Tree, or Artificial Neural Networks—has demonstrated superior accuracy and robustness in predicting non-linear spatial transitions (Gharaibeh et al. 2020; Aksoy 2024; Tahir et al. 2025). Moreover, integrating Agent-Based Models (ABM) can capture the influence of individual or institutional behaviors on land change processes, offering a more dynamic and behaviorally realistic representation of landscape evolution (Hussain et al. 2025). Enhancing data resolution and diversity, through multi-sensor and multi-temporal datasets, will further refine transition probabilities and minimize uncertainty in long-term projections.

Additionally, incorporating climate change projections and socio-economic indicators—including population growth, infrastructure expansion, and land tenure—will allow more comprehensive and policy-relevant modeling frameworks. These directions will align LULC modeling with the broader goals of sustainable land management, ecosystem resilience, and adaptive urban planning. Ultimately, while the CA–Markov model remains a proven and accessible method for regional-scale LULC forecasting, its predictive capacity can be substantially strengthened through multi-model integration, stakeholder-informed scenario testing, and the use of higher-resolution remote sensing datasets.

Acknowledgements The authors would like to thank General Directorate of Turkish Forestry for forest cover type maps.

Author contributions S.K: conceptualization, methodology, writing – original draft, writing – review and editing. F.S: methodology, writing – original draft, writing – review and editing, A.G: methodology, writing – original draft, writing – review and editing.

Funding There is no funding.

Data availability The datasets are available on reasonable request.

Declarations

Conflict of interest The authors declare that they have no known competing financial interests or personal relationships that could have appeared to influence the work reported in this paper.

References

Aksoy H (2024) Evaluation of forest areas and land use/cover (LULC) changes with a combination of remote sensing, intensity analysis and CA-Markov modelling. N Z J for Sci 54:20. https://doi.org/10.33494/nzjfs542024x328x

Aksoy H, Kaptan S (2020) Simulation of future forest and land use/cover changes (2019–2039) using the cellular automata-Markov model. Geocarto Int 37(4):1183–1202. https://doi.org/10.1080/10106049.2020.1778102

Aksoy H, Kaptan S (2021) Monitoring of land use/land cover changes using GIS and CA-Markov modeling techniques: a study in Northern Turkey. Environ Monit Assess 193:507. https://doi.org/10.1007/s10661-021-09281-x

Aksoy H, Kaya S, Duran Z (2022) Spatio-temporal dynamics of LULC changes using the CA-Markov model: a case study of Istanbul. Sustain Cities Soc 75:103456

Aliani H, Malmir M, Sourodi M, Kafaky SB (2019) Change detection and prediction of urban land use changes by CA–Markov model (case study: Talesh County). Environ Earth Sci 78:546. https://doi.org/10.1007/s12665-019-8557-9

Alsharif M, Alzandi AA, Shrahily R, Mobarak B (2022) Land use land cover change analysis for urban growth prediction using Landsat satellite data and Markov chain model for Al Baha Region Saudi Arabia. Forests 13(10):1530. https://doi.org/10.3390/f13101530

Aniah P, Bawakyillenuo S, Codjoe SNA, Dzanku FM (2023) Land use and land cover change detection and prediction based on

CA-Markov chain in the savannah ecological zone of Ghana. Environ Challenges 10:100664. https://doi.org/10.1016/j.envc.2022.100664

Anonymous (2020) Ankara Orman Bölge Müdürlüğü, Çankırı Orman İşletme Müdürlüğü, Merkez işletme şeflikliği, fonksiyonel orman amenajman planı, Orman Genel Müdürlüğü, Orman İdaresi ve Planlama Dairesi, Ankara

Asif M, Kazmi JH, Tariq A, Zhao N, Guluzade R, Soufan W, Almutairi KF, Sabagh AE, Aslam M (2023) Modelling of land use and land cover changes and prediction using CA-Markov and random forest. Geocarto Int 38(1):2210532. https://doi.org/10.1080/10106049.2023.2210532

Bagaria P, Nandy S, Mitra D, Sivakumar K (2021) Monitoring and predicting regional land use and land cover changes in an estuarine landscape of India. Environ Monit Assess 193(3):124. https://doi.org/10.1007/s10661-021-08915-4

Behera A, Rawat KS, Kumar S, Almuflih AS, Almakayeel N, Qureshi MRN (2025) Simulation and projection of land use and land cover using remote sensing data and CA–Markov model case study. Geocarto Int 40(1):2450441. https://doi.org/10.1080/10106049.2025.2450441

Belay H, Melesse AM, Tegegne G (2024) Scenario-based land use and land cover change detection and prediction using the cellular automata–Markov model in the GumaraWatershed, Upper Blue Nile Basin, Ethiopia. Land 13(3):396. https://doi.org/10.3390/land13030396

Beroho M, Briak H, Cherif EK, Boulahfa I, Ouallali A, Mrabet R, Kebede F, Bernardino A, Aboumaria K (2023) Future scenarios of land use/land cover (LULC) based on a CA-Markov simulation model: case of a Mediterranean Watershed in Morocco. Remote Sens 15:1162. https://doi.org/10.3390/rs15041162

Blaschke T (2010) Object based image analysis for remote sensing. ISPRS J Photogramm Remote Sens 65(1):2–16

Congalton RG (1991) A review of assessing the accuracy of classifications of remotely sensed data. Remote Sens Environ 37(1):35–46

Foley JA, DeFries R, Asner GP, Barford C, Bonan G, Carpenter SR, Chapin FS, Coe MT, Daily GC, Gibbs HK, Helkowski JH, Holloway T, Howard EA, Kucharik CJ, Monfreda C, Patz JA, Prentice IC, Ramankutty N, Snyder PK (2005) Global consequences of land use. Science 309(5734):570–574. https://doi.org/10.1126/science.1111772

Foody GM (2002) Status of land cover classification accuracy assessment. Remote Sens Environ 80(1):185–201. https://doi.org/10.1016/S0034-4257(01)00295-4

Fu F, Deng S, Liu W, Bai Z (2022) Research on the spatiotemporal evolution of land use landscape pattern in a county area based on CA-Markov model. Sustain Cities Soc 80:103760. https://doi.org/10.1016/j.scs.2022.103760

Ghalehteimouri KJ, Shamsoddini A, Mousavi MN, Binti F, Ros C, Khedmatzadeh A (2022) Predicting spatial and decadal of land use and land cover change using integrated cellular automata Markov chain model based scenarios (2019–2049) Zarriné-R ū d River Basin in Iran. Environ Challenges 6:100399. https://doi.org/10.1016/j.envc.2021.100399

Gharaibeh A, Shaamala A, Obeidat R, Al-Kofahi S (2020) Improving land-use change modeling by integrating ANN with Cellular Automata-Markov Chain model. Heliyon 6:e05092. https://doi.org/10.1016/j.heliyon.2020.e05092

Halmy MWA, Gessler PE, Hicke JA, Salem BB (2015) Land use/land cover change detection and prediction in the north-western coastal desert of Egypt using Markov-CA. Appl Geogr 63:101–112. https://doi.org/10.1016/j.apgeog.2015.06.015

Hamad R, Balzter H, Kolo K (2018) Predicting land use/land cover changes using a CA-Markov model under two different scenarios. Sustainability 10:3421. https://doi.org/10.3390/su10103421

Hind M, M'hammed S, Akziz D, Zoubida N (2022) Assessment of land use–land cover changes using GIS, remote sensing, and CA–Markov model: a case study of Algiers, Algeria. Appl Geomat 14:811–825. https://doi.org/10.1007/s12518-022-00472-w

Huang Y, Yang B, Wang M, Liu B, Yang X (2020) Analysis of the future land cover change in Beijing using CA–Markov chain model. Environ Earth Sci 79:60. https://doi.org/10.1007/s12665-019-8785-z

Hussain S, Qaisrani SA, Tariq A, Mubeen M, Ullah S (2025) Assessing past, present, and simulated future prediction of land use land cover changes using CA-Markov chain models with Satellite data. Results Eng 26:105585. https://doi.org/10.1016/j.rineng.2025.105585

Jana A, Jat MK, Saxena A, Choudhary M (2022) Prediction of land use land cover changes of a river basin using the CA-Markov model. Geocarto Int 37(26):14127–14147. https://doi.org/10.1080/10106049.2022.2086634

Karimi H, Jafarnezhad J, Khaledi J, Ahmadi P (2018) Monitoring and prediction of land use/land cover changes using CA-Markov model: a case study of Ravansar County in Iran. Arab J Geosci 11:592. https://doi.org/10.1007/s12517-018-3940-5

Kavathekar V, Tripathy AK, Chettri SK (2025) Spatio-temporal urban land use change in Mumbai, India: analysis and prediction of 2030 using satellite data and a cellular automata-Markov chain model. Int J Geoinf 21(5):80–94. https://doi.org/10.52939/ijg.v21i5.4163

Khwarahm NR, Najmaddin PM, Ararat K, Qader S (2021) Past and future prediction of land cover land use change based on earth observation data by the CA–Markov model: a case study from Duhok governorate. Iraq Arabian J Geosci 14:1544. https://doi.org/10.1007/s12517-021-07984-6

Kumar S, Radhakrishnan N, Mathew S (2014) Land use change modelling using a Markov model and remote sensing. Geomat Nat Hazards Risk 5(2):145–156. https://doi.org/10.1080/19475705.2013.795502

Lambin EF, Geist HJ, Lepers E (2001) Dynamics of land-use and land-cover change in tropical regions. Annu Rev Environ Resour 28(1):205–241. https://doi.org/10.1146/annurev.energy.28.050302.105459

Lu D, Weng Q (2007) A survey of image classification methods and techniques for improving classification performance. Int J Remote Sens 28(5):823–870

Mansour S, Al-Belushi M, Al-Awadhi T (2020) Monitoring land use and land cover changes in the mountainous cities of Oman using GIS and CA-Markov modelling techniques. Land Use Policy 91:104414. https://doi.org/10.1016/j.landusepol.2019.104414

Masalvad SS, Patil C, Pravalika A, Katageri B, Bekal P, Patil P, Hegde N, Sahoo UK, Sakare PK (2024) Application of geospatial technology for the land use/land cover change assessment and future change predictions using CA Markov chain model. Environ Dev Sustain 26:24817–24842. https://doi.org/10.1007/s10668-023-03657-4

Mathewos M, Lencha SM, Tsegaye M (2022) Land use and land cover change assessment and future predictions in the Matenchose Watershed, Rift Valley Basin, using CA-Markov simulation. Land 11(10):1632. https://doi.org/10.3390/land11101632

Mondal MS, Sharma N, Garg PK, Kappas M (2016) Statistical independence test and validation of CA Markov land use land cover (LULC) prediction results. The Egyptian J Remote Sens Space Sci 19(2):259–272. https://doi.org/10.1016/j.ejrs.2016.08.001

Moradi F, Kaboli HS, Lashkarara B (2020) Projection of future land use/cover change in the Izeh-Pyon Plain of Iran using CA-Markov model. Arab J Geosci 13:998. https://doi.org/10.1007/s12517-020-05984-6

Nagasa MD, Edosa BT (2024) Predicting spatiotemporal forest cover dynamics using the CA-Markov model in the Chuta Gorgis Forest between 1983 and 2050. J Inf Anal 2:9. https://doi.org/10.53964/jia.2024009

Nasehi S, Namin AI, Salehi E (2019) Simulation of land cover changes in urban area using CA-MARKOV model (case study: zone 2 in Tehran, Iran). Model Earth Syst Environ 5(1):193–202. https://doi.org/10.1007/s40808-018-0527-9

Nouri J, Gharagozlou A, Arjmandi R, Faryadl S, Adl M (2014) Predicting urban land use changes using a CA–Markov model. Arab J Sci Eng 39:5565–5573. https://doi.org/10.1007/s13369-014-1119-2

Rahnama MR (2021) Forecasting land-use changes in Mashhad Metropolitan area using Cellular Automata and Markov chain model for 2016–2030. Sustain Cities Soc 64:102548. https://doi.org/10.1016/j.scs.2020.102548

Roy DP, Wulder MA, Loveland TR, Ce W, Allen RG, Anderson MC, Zhu Z (2014) Landsat-8: science and product vision for terrestrial global change research. Remote Sens Environ 145:154–172. https://doi.org/10.1016/j.rse.2014.02.001

Ruben GB, Zhang K, Dong Z, Xia J (2020) Analysis and projection of land-use/land-cover dynamics through scenario-based simulations using the CA-Markov model: a case study in Guanting Reservoir Basin, China. Sustainability 12(9):3747. https://doi.org/10.3390/su12093747

Singh SK, Laari PB, Mustak S, Srivastava PK, Szabó S (2018) Modelling of land use land cover change using earth observation datasets of Tons River Basin, Madhya Pradesh, India. Geocarto Int 33:1202–1222

Song C, Woodcock CE, Seto KC, Lenney MP, Macomber SA (2001) Classification and change detection using Landsat TM data: when and how to correct atmospheric effects? Remote Sens Environ 75(2):230–244

Subedi P, Subedi K, Thapa B (2013) Application of a hybrid cellular automaton – Markov (CA-Markov) model in land-use change prediction: a case study of Saddle Creek Drainage Basin, Florida. Appl Ecol Environ Sci 1(6):126–132

Tadese S, Soromessa T, Bekele T (2021) Analysis of the current and future prediction of land use/land cover change using remote sensing and the CA-Markov model in Majang Forest Biosphere Reserves of Gambella, Southwestern Ethiopia. Sci World J 2021:6685045. https://doi.org/10.1155/2021/6685045

Tahir Z, Haseeb M, Mahmood SA, Batool S, Al-Wadud MA, Ullah S, Tariq A (2025) Predicting land use and land cover changes for sustainable land management using CA-Markov modelling and GIS techniques. Sci Rep 15:3271. https://doi.org/10.1038/s41598-025-87796-w

Tali JA, Divya S, Murthy K (2013) Influence of urbanization on the land use change: a case study of Srinagar City. Am J Res Comm 1:271–283

Tariq A, Yan J, Mumtaz F (2022) Land change modeler and CA-Markov chain analysis for land use land cover change using satellite data of Peshawar, Pakistan. Phys Chem Earth 128:103286. https://doi.org/10.1016/j.pce.2022.103286

Turner BL, Lambin EF, Reenberg A (2007) The emergence of land change science for global environmental change and sustainability. Proc Natl Acad Sci U S A 104(52):20666–20671. https://doi.org/10.1073/pnas.0704119104

Wang SW, Munkhnasan L, Lee WK (2021) Land use and land cover change detection and prediction in Bhutan's high altitude city of Thimphu, using cellular automata and Markov chain. Environ Challenges 2:100017. https://doi.org/10.1016/j.envc.2020.100017

Weslati O, Bouaziz S, Sarbeji MM (2023) Modelling and assessing the spatiotemporal changes to future land use change scenarios using remote sensing and CA-Markov model in the Mellegue Catchment. J Indian Soc Remote Sens 51(1):9–29. https://doi.org/10.1007/s12524-022-01618-4

Wulder MA, White JC, Goward SN, Masek JG, Irons JR, Herold M, Woodcock CE (2008) Landsat continuity: issues and opportunities for land cover monitoring. Remote Sens Environ 112(3):955–969

Yulianto F, Maulana T, Khomarudin MR (2019) Analysis of the dynamics of land use change and its prediction based on the integration of remotely sensed data and CA-Markov model, in the upstream Citarum Watershed, West Java, Indonesia. Int J Digit Earth 12(10):1151–1176. https://doi.org/10.1080/17538947.2018.1497098

Zhu Z, Woodcock CE (2014) Continuous change detection and classification of land cover using all available Landsat data. Remote Sens Environ 144:152–171